Blends in Two Dimensions: Mixtures of a Ferroelectric Liquid Crystalline Copolymer with Its Side-Chain Monomer at the Air-Water Interface

A. F. Thibodeaux, U. Rädler, R. Shashidhar,† and R. S. Duran*

Center for Macromolecular Science and Engineering, Department of Chemistry, University of Florida, Gainesville, Florida 32611-2046

Received April 27, 1993; Revised Manuscript Received September 14, 1993®

ABSTRACT: In an attempt to adjust the lateral density of monolayer and multilayer films of a ferroelectric liquid crystalline copolymer, blends of the copolymer were made with the corresponding mesogenic monomer unit. The monomer was chosen as the second component since it forms monolayer films which are more condensed than the copolymer and because of its miscibility with the structurally similar copolymer. Analysis of the interaction between the molecules of the mixed monolayers included Π-area isothermal data, calculation of the excess ΔG_{mix}, thermal dependence of isotherms, and Brewster angle microscopy. On the basis of these results, the films appear to be completely miscible over all conditions presented and the blend monolayer films are more condensed than the pure copolymer films.

Introduction

Mixed monolayers have been studied since the advent of Langmuir-Blodgett film research, and mixed films were reported in the literature in the early 1920s.[1,2] Ries and co-workers published results from blends of fatty acids with polymers in 1961; and Gaines' manuscript[3] devotes a whole chapter to thermodynamics and a discussion of mixed monolayers. More recently, Gabrielli and co-workers have rigorously investigated the behavior of various combinations of polymers and low molecular weight materials in monolayer blends.[4-6] Considerably less work has been performed on the behavior of liquid crystalline (LC) materials as monolayers.[7] Ringsdorf and co-workers have presented studies in this area which indicate that a self-ordering moiety, such as a LC mesogen, incorporated into the side chain of a polymer enhances ultimate ordering in the built-up multilayer film.[8]

Miscibility of a liquid crystalline (LC) polymer and monomer in the bulk state has been the topic of several studies of late. Although initial studies on nematics showed that generally the miscibility between a liquid crystalline polymer and monomer is poor, more recent studies on a ferroelectric (FE) LC copolymer mixed with a FE LC monomer showed good miscibility over a major portion of the phase diagram. These studies led to two important results: (a) the ferroelectric smectic C* phase was found to be miscible at all proportions in the temperature-concentration plane and (b) the ferroelectric properties in the bulk state could be tuned continuously as a function of composition. In this paper we have investigated the monolayer behavior of a similar copolymer-monomer blend (Figure 1) at the air-water interface.

The monolayer and multilayer behavior of the side-chain FE LC copolymer, denoted as 10PPB2-CO, has been previously investigated.[9] In harnessing thin film ferroelectric properties, it is important to have films that are both thermally stable and ordered with respect to mesogen orientation. The goal of previous research was to produce such organized films of 10PPB2-CO by the Langmuir-Blodgett deposition technique since this copolymer forms stable monolayers on a water surface. Prior work has also shown that 10PPB2-CO can be deposited onto hydrophobic substrates, by both conventional and alternate deposition techniques, to produce what appear to be *y*-type and *x*-type films, respectively.[9] However, small-angle x-ray scattering (SAXS) data from both types of multilayer films yield an identical layer spacing of approximately 47 Å. Considering the calculated extended length of the side-chain group including the siloxane backbone is only 42 Å, the data indicate that the transferred monolayers rearrange to form an interdigitated layer structure, much like that seen in the bulk. This rearrangement upon multilayer formation thus limits control over the packing density and stacking sequences attainable in these films.

The monomer (10PPB2) was chosen as a blending candidate to alter the films of 10PPB2-CO for two reasons. First, as previously stated the copolymer and the monomer have been shown to be completely miscible over all concentrations in the bulk;[10] therefore, miscibility in the monolayers is favorable. Second, 10PPB2 is crystalline in the bulk phase at room temperature and forms more closely-packed Langmuir films than the copolymer. Therefore, it appears to be a suitable mixing material to reduce the mobility and surface area of the side-chain groups in 10PPB2-CO monolayers.

Several methods were employed to determine miscibility in the monolayers. Conventional data analysis, such as compressibility and collapse pressure trends with blend composition, isobaric data of mean molecular area versus blend concentration, calculation of the excess free energy of mixing (ΔG_{mix}^{xs}), and thermal dependence studies of blend isotherms, are presented and discussed.[3-6,11-15] Investigations on the morphology of the blended monolayers are presented in the form of Brewster angle micrographs and reflected intensity studies.[16,17] Using a commercially available instrument, the blends films were recorded during compression and analyzed. Additionally, the use of an analyzer placed in front of the camera allowed information concerning the orientational order of the molecules at the surface to be obtained.

Experimental Section

The syntheses of 10PPB2-CO and 10PPB2 are described in detail elsewhere.[18]

Spreading solutions were 0.5-1.0 mg/mL and were made in spectrograde chloroform (Kodak). Blend solutions were made from two stock solutions of 10PPB2 and 10PPB2-CO. Mole ratios

† Center for Bio/Molecular Science and Engineering, Naval Research Laboratory, Code 6900, Washington, DC 20375-5348.

® Abstract published in *Advance ACS Abstracts*, November 15, 1993.

0024-9297/94/2227-0784$04.50/0

10PPB2-CO

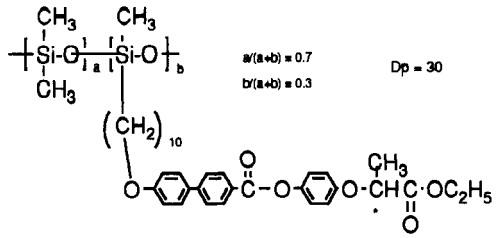

10PPB2

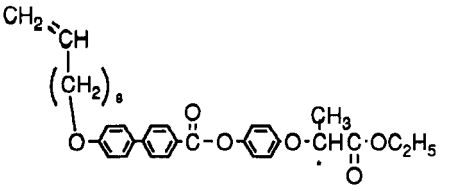

Figure 1. Structure of 10PPB2-CO and 10PPB2 (monomer).

were determined and converted into volumes for each component in the blend. Solutions were made using a 1-mL Hamiltonian gas-tight syringe to deliver the appropriate volumes.

Isotherms. Experiments were performed at 25 ± 0.5 °C unless otherwise noted. Films were spread on a pure water subphase obtained by deionization followed by polishing through a 5-bowl Milli-Q Plus system (>18 MΩ) from Millipore Corp. Isotherms of all materials and blends studied were reproducible within ±0.1 Å^2. Monolayer films were compressed at a speed of 2 Å^2/molecule·min. This rate was determined to be below the range in which any of the isotherms showed measurable rate dependence. Mean molecular areas refer to the average surface area per mesogenic repeat unit in the case of 10PPB2-CO unless otherwise specified and the average surface area per molecule in the case of 10PPB2.

The Langmuir–Blodgett trough used was a computer-interfaced LB5000 (KSV Instruments, Helsinki, Finland), with a dual barrier system (compression from both ends toward the center) and a Wilhelmy film balance with carefully prewetted platinum or filter paper plates.

Integration of surface pressure versus surface area (Π–A) isotherms was accomplished using KSV LB5000 analytical software provided with the instrument. ΔG_{mix}^{xs} values were integrated from a lower pressure limit of 0.3 mN/m to eliminate errors included in values caused by fluctuations in the base line. Collapse pressures were determined by analyzing derivative isotherm curves ($d\Pi/dA$) which were smoothed by a seven-point smoothing routine and taking the minimum derivative value as the collapse surface area. Corresponding collapse pressures were then taken from the original isotherms.

Brewster Angle Microscopy. The Brewster angle microscope used was a BAM1 from Nanofilm Technologie Gmbh (Göttingen, Germany). A He–Ne laser (p-polarized) was used as the light source. The angle of incidence was initially set to 53° and then adjusted to minimize the reflected intensity of the clean water surface prior to spreading of each film. All photos presented were taken with a rotatable analyzer set at 90° placed in between the reflected signal and the CCD camera. A frame-grabbing program (Videopix, Sun Microsystems) was used to generate photos from videotape and convert them to a computer-readable format. BAM intensity ratios were obtained by integrating the intensities over all pixels of the captured image for the clean water surface, I_0, and for the film as compressed, I. In the intensity versus surface area plots for the blends (Figure 14), all instrument settings including intensity gain were held constant, for the purpose of comparison.

Results and Discussion

The copolymer and monomer studied in this work have been previously studied in the bulk state and at the air–water interface.[9,18–21] The thermotropic polymorphism for the bulk monomer and copolymer is shown in Figure 2. The 10PPB2-CO copolymer is in a liquid crystalline state at room temperature, unlike the monomer whose smectic C (S_C*) phase is at elevated temperatures. Both the copolymer and monomer contain a chiral center in the mesogenic group, show a chiral S_C* mesophase, and under certain conditions exhibit ferroelectric properties.[18]

Isotherms. Monolayer film behavior of the monomer, 10PPB2, has been documented in detail elsewhere.[20] The thermal dependence of this monomer is shown in Figure

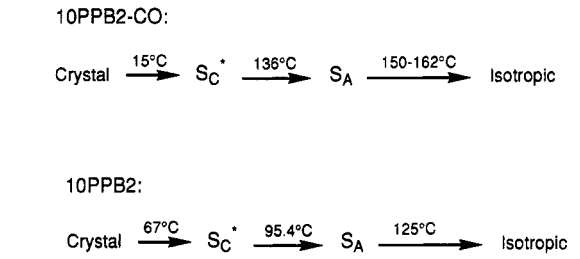

Figure 2. Thermal behavior of the copolymer and monomer.

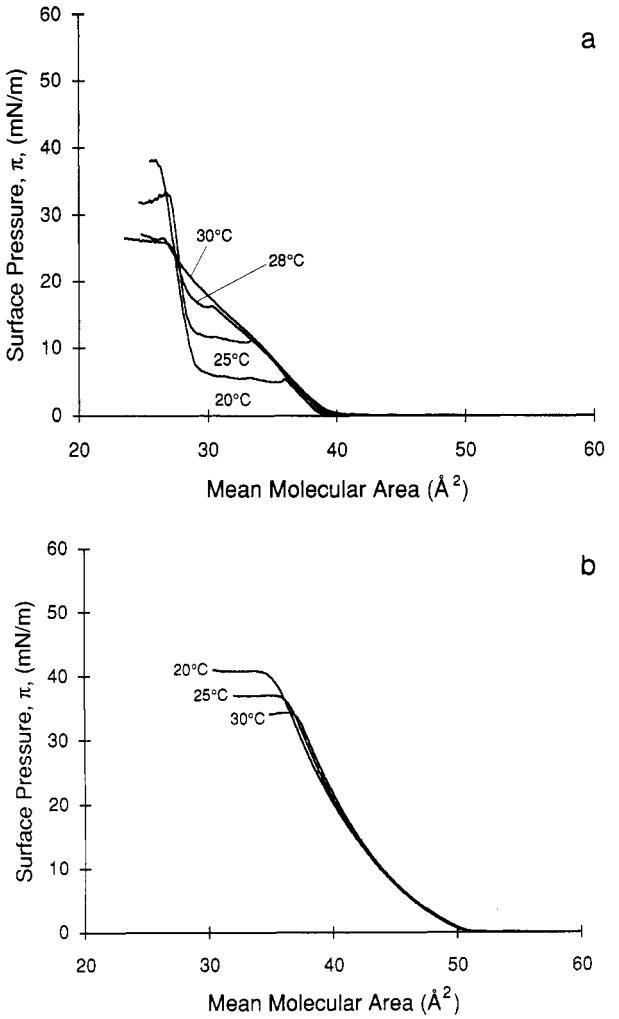

Figure 3. Isotherms of 10PPB2 (monomer) (a) and 10PPB2-CO (b) at various temperatures.

3a and agrees with previous findings of Rettig and coworkers.[20] On the basis of Brewster angle microscopy and hysteresis experiments, it was determined that the monomer exists as an ordered fluid phase below the transition region and exhibits birefringent behavior consistent with long-range orientational correlations between mesogens. Above the transition pressure, the monomer film is a highly incompressible solid film and has a surface area consistent

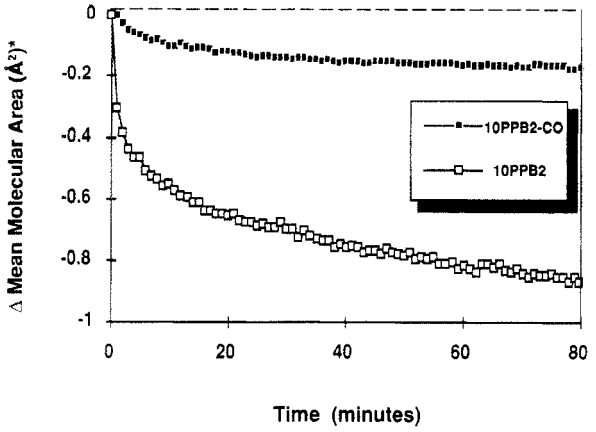

Figure 4. Constant pressure measurements of mean molecular area versus time for 10PPB2 and 10PPB2-CO at 10 mN/m and 25 °C.

with close packing of the mesogen.[22] It is apparent from the isotherms that small changes in temperature over the range of 20–30 °C drastically affect the behavior of the monomer monolayer in the transition region. However, the compressibility and surface area of the less condensed phase at a given pressure are not highly temperature dependent.

For comparison, the thermal dependence of the copolymer over the same temperature range is shown in Figure 3b. Comparing the copolymer and monomer isotherms, the copolymer is in a significantly more expanded state. Since the collapse point of the copolymer is only slightly smaller than the onset point of pressure increase in the monomer films, it can be asserted that the side-chain groups of the copolymer are not close packed at collapse. Relative to the monomer, the copolymer is more stable over all pressures below collapse as shown in the plot of the change in surface area versus time at constant pressure in Figure 4. It is also resistant to change with temperature over the range shown (Figure 3b). Hysteresis curves, generated by compressing over collapse pressure with subsequent reexpansion and recompression, show reversible collapse[23] and fluid film behavior.[9,22] Previous work by Adams et al. demonstrated that the equilibrium "collapse" pressure, corresponding to the inflection point of the curve at high pressure, was a transition of liquid crystalline monolayer to bulk liquid crystalline material in equilibrium with the monolayer.[22]

Blends. Isotherms of 10PPB2/10PPB2-CO blends with monomer concentrations of 20, 30, 50, and 70% (mol %) at different temperatures are shown in Figure 5a–d. The influence of the monomer content in the form of a phase transition is more evident in the blends at lower temperatures and at a higher concentration of monomer. There is no apparent transition region throughout the temperature range for the 20% concentration (mol %) 10PPB2 (Figure 5a). This may indicate that at these concentrations the polymer content is still effective in disrupting lateral ordering or crystallization of the monomer and copolymer side groups. At 30% 10PPB2 composition the isotherms exhibit similar behavior to that of the copolymer and 20% mixture; however, a shoulder appears in the 30% curve at 20 °C. Under these conditions, the film could be compressed to pressures significantly above the calculated

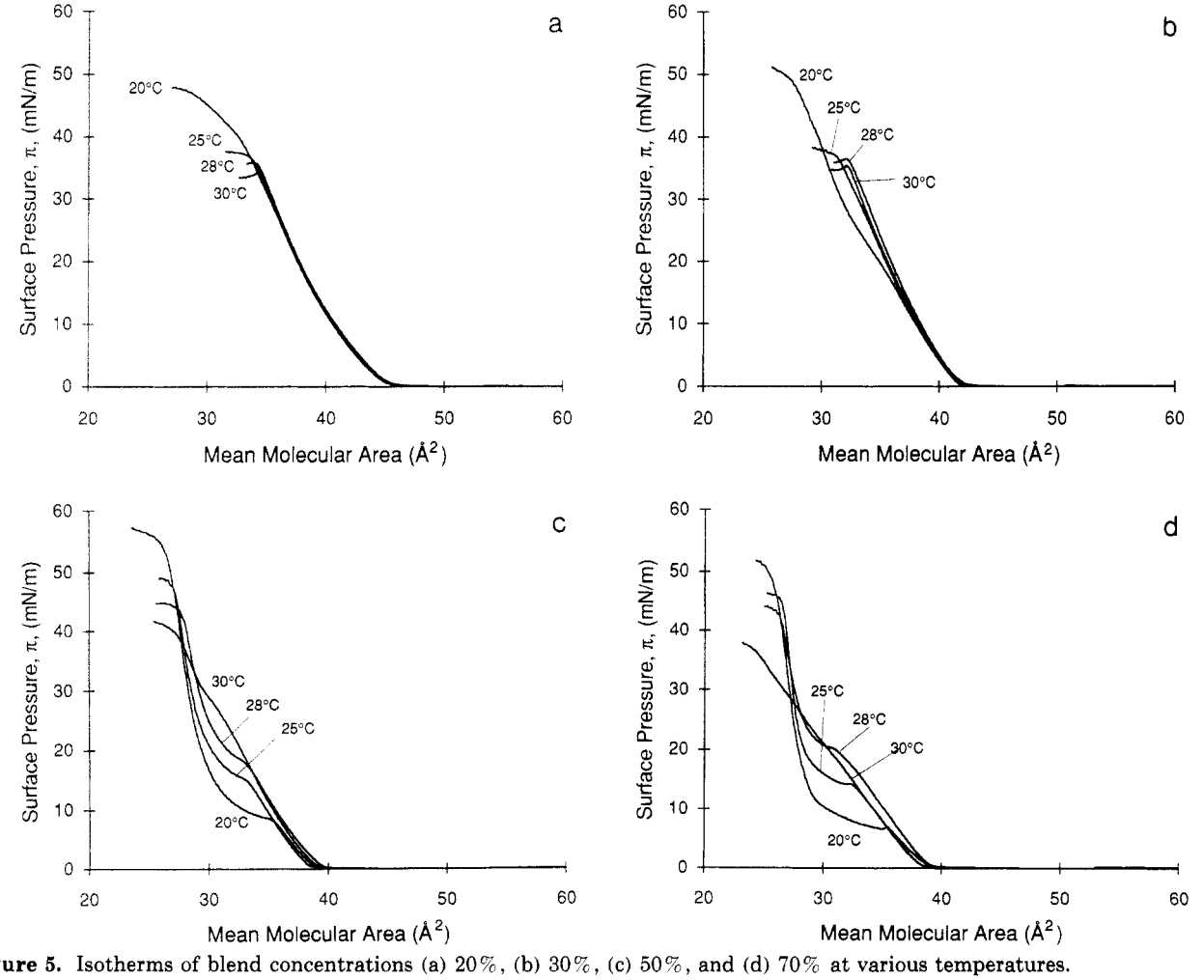

Figure 5. Isotherms of blend concentrations (a) 20%, (b) 30%, (c) 50%, and (d) 70% at various temperatures.

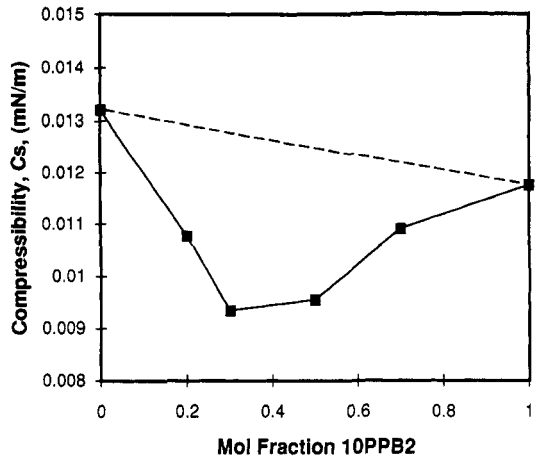

Figure 6. Compressibility, C_s, versus blend composition at 5 mN/m and 25 °C.

collapse point. Although the 50% and 70% monomer blends resemble the general shape of the monomer isotherm curves, they show an increase in the pressure and a decrease in the width of the transition region with decreasing monomer content. The added copolymer causes the liquid analogous phase to persist at higher surface pressures much like increasing the temperature in the case of the pure monomer. The 50% and 70% compositions can also be overcompressed to pressures well above the collapse point, as was seen in the 30% film at 20 °C. This phenomenon may be caused by cocrystallization of the polymer side-chain groups with monomer under these conditions, with the underlying polymer backbone "strengthening" the monolayer and inhibiting the collapse process.

Compressibility and Collapse of Blend Monolayers. The above observations indicate that the pure components may be miscible because the isotherm features are not additive of the pure component isotherms and vary continuously with composition. However, they are not necessarily conclusive, and a more detailed analysis is necessary. According to Crisp[24] and Gaines,[25] a composition-dependent decrease in compressibility from additive values and a continuous variation of collapse pressures of mixed films with composition are both indications of miscibility. The compressibility of a monolayer film, C_s, may be described as follows:

$$C_s = -1/A(dA/d\Pi)$$

where $dA/d\Pi$ is the inverse slope of the isotherm at surface area A. Compressibility data were analyzed versus blend composition, and an example taken at 25 °C is shown in Figure 6. Similar compressibility behavior was seen at other temperatures in the range 20–30 °C. The results for pressures higher than 10 mN/m are not included because anomalously high compressibilities are obtained in the transition regions present in some of the isotherms. Intimate mixing of a blend film would theoretically produce stronger interactions between monolayer components, creating a more coherent and condensed film and consequently decreasing film compressibility. The 10PPB2-CO/10PPB2 blend films show a decreased compressibility from additivity of the pure films, which indicates miscibility as well as attractive interactions between components.

According to Gaines,[25] in the case of total immiscibility, a mixed film will collapse at the pressure of the less stable component, while the collapse pressures of miscible mixtures vary continuously with composition (often showing a positive or negative deviation from linearity).

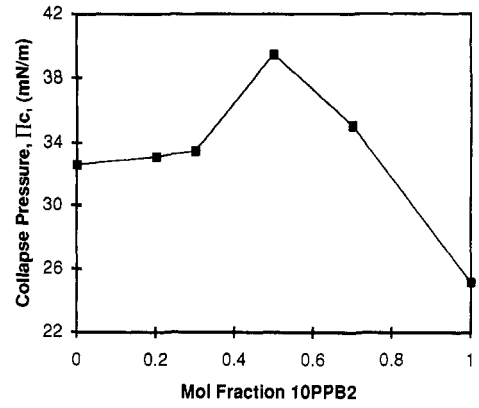

Figure 7. Collapse pressure, π_c, versus blend composition at 25 °C. Surface pressures are 5 (■), 10 (●), and 20 mN/m (▲).

This is explained by application of the Phase Rule as put forth by Crisp.[24] In the case of an immiscible monolayer film with two coexisting phases at collapse, the degrees of freedom are reduced to zero, resulting in the invariance of collapse pressure with composition. If the system is miscible, i.e., one monolayer phase at collapse, the degree of freedom is 1, and there will be a continuous variation of collapse pressure with concentration of one blend compound.

Although the collapse pressure is often equated with equilibrium spreading pressure (ESP), the processes are very different. Collapse may be dependent upon kinetic factors such as concentration and compression speed, while equilibrium spreading pressure is independent of both. While an ESP has not been observed for either pure component, equilibrium values have been approached by reducing barrier speed and concentration until no further change in the isotherm is detected. However, overcompression of the monolayer (beyond ESP) is almost certain. The copolymer, on the other hand, shows a collapse very close to the theoretical ESP but represents a transition from liquid crystalline monolayer to a bulk liquid crystalline phase.[22] Because of this behavior, reproducibility of monomer and blend isotherms, and the care in which collapse was determined, the data analysis is believed valid, though only qualitative interpretations can be drawn.

The actual collapse pressures of the monolayers are not necessarily evident from the isotherm curves. However, an accepted determination of the collapse is the minimum of the isotherm derivative curve, or the point of inflection where the slope of the isotherm begins to increase at the higher pressures.[25] This method was employed to determine the collapse of all blend compositions as presented in Figure 7. The plot of Π_c versus monomer concentration shows a continuous variation with composition, indicating a completely miscible system. Similar continuous variations with composition were obtained from collapse pressure data at other temperatures in the range 20–30 °C.

Thermodynamics of Mixing in the Monolayer Blends. The qualitative analysis of the isotherm behavior presented above is a useful indication of miscibility but cannot describe the types of interactions, the extent of interaction, or whether partial demixing occurs. To evaluate more quantitatively the ease of mixing or interactions between the components, thermodynamic analysis of the isothermal data is often used.[4-6,11,15] When considering the thermodynamic behavior of monolayers, Π–A isotherms may be viewed as the two-dimensional analog of a pressure–volume isotherm curve for a three-dimensional system. The obvious difference is that, since a pressure is applied mechanically during compression,

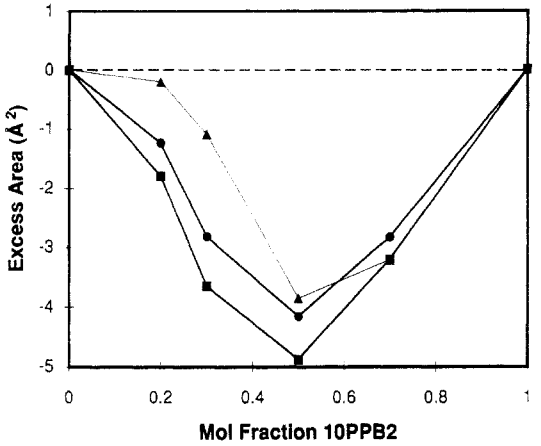

Figure 8. ΔA_{xs} versus blend concentration of 10PPB2 at 25 °C. Surface pressures are (■), 10 (●), and 20 mN/m (▲).

the conditions of an experiment are often not at equilibrium. However, at low compression rates, isotherms can be used to evaluate the extent of interaction and miscibility of the monolayer blend components. The compression rate in the isotherms shown was 2 Å²/molecule (or repeat unit)·min and was found to be well below compression rates where speed dependence of the isotherms is observed.

By far the most commonly used indication for miscibility is the analysis of surface area values at constant pressure versus blend composition. An alternative area value presentation is that of excess surface area versus concentration of one blend component. The excess area values represent the difference in packing efficiency of the blend components over the additive mixing values. The excess area, ΔA_{xs} is given as follows:

$$\Delta A_{xs} = A - (c_1A_1 + c_2A_2)$$

where A is the surface area of the blend at a given surface pressure, c_1 and c_2 are the mole fractions, and A_1 and A_2 are the surface areas of components 1 and 2, respectively. It becomes clear that ΔA_{xs} is simply the difference in area of a particular blend composition as compared with the calculated ideal mixing area (contained in the two terms within the parentheses). A plot of ΔA_{xs} for the 10PPB2-CO/10PPB2 blends at 25 °C is shown in Figure 8. When determining the miscibility of blends, a linear relationship at or around zero almost always indicates phase separation with a large domain size. For a miscible system, negative excess area values are expected, while positive values are usually a clear sign of phase separation. Since a negative deviation is evident in all curves shown, intimate mixing is inferred.[3,13,26]

To describe the extent of interaction between the blend materials, it is useful to look at the excess ΔG of mixing.[13,14] For a two-component blend system, this is described according to the Goodrich method[27] as applied by Bacon and Barnes[13] as follows:

$$\Delta G_{mix}^{xs,\pi} = \int_0^{\pi}(A - c_1A_1 - C_2A_2)\,d\pi$$

The value in the parentheses is ΔA_{xs}. ΔG_{mix}^{xs} for an ideal system is equal to zero where there is no interaction between the individual components. In the case of any miscibility of the system, ΔG_{mix}^{xs} will have a negative value.

To calculate ΔG_{mix}^{xs} by the integration method of Goodrich, the path of the isotherm is assumed to be reversible. For the monomer and blend monolayers which show a transition region, reversibility of the isotherm was experimentally confirmed below the transition pressure. Therefore, ΔG_{mix}^{xs} data will be presented for pressures below the transition, which vary according to the composition and temperature being discussed.

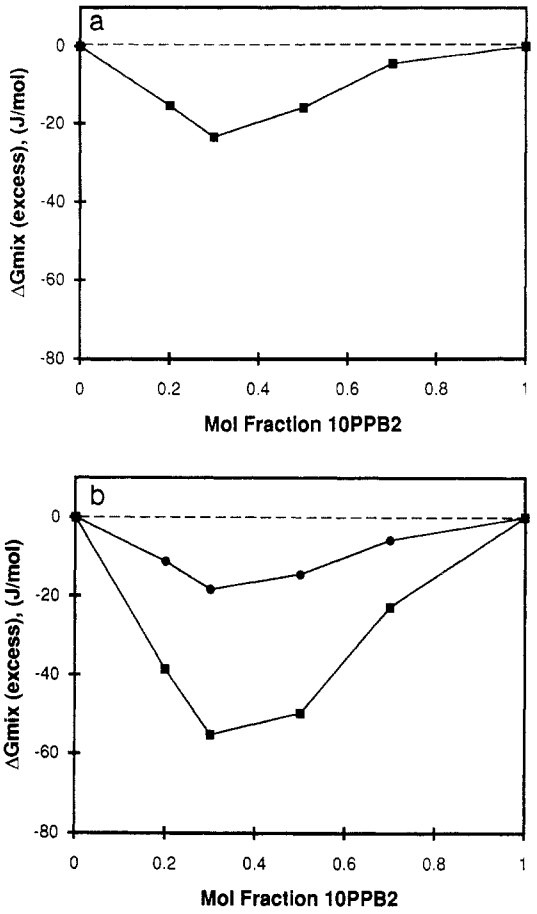

Figure 9. ΔG_{mix}^{xs} versus blend concentration of 10PPB2 at (a) 20 and (b) 25 °C. Surface pressures are 5 (■) and 10 mN/m (●).

In Figure 9, ΔG_{mix}^{xs} values versus composition are plotted for 20 and 25 °C. While in the excess area plots from Figure 8 pressures up to 20 mN/m are shown, pressures for the ΔG_{mix}^{xs} values are limited to those below the transition region for all compositions under these conditions for the reasons stated above. All values presented show a small but significant negative deviation from zero, and their magnitudes are similar to data reported on other miscible monolayer blend systems in the literature.[13]

A notable feature of the ΔA_{xs} values versus the corresponding ΔG_{mix}^{xs} is that the minimum of the curves is shifted right in the ΔA_{xs} plots. Most of the ΔG_{mix}^{xs} curves appear to have minima somewhere close to 40%, while the ΔA_{xs} plots are either centered at 50% or skewed to higher concentrations. This may be explained by the difference in origin of these values. The ΔA_{xs} data are taken at a given point on the isotherm curve and are path-independent values. They represent the final efficiency in packing of the two components at a given pressure. However, ΔG_{mix} values are integrated as the area under the isotherm and are highly dependent on the shape of the isothermal curve. These values represent the spontaneity or "ease" of mixing up to a given pressure value. The shift of the ΔG_{mix}^{xs} minima left of the corresponding ΔA_{xs} values under the same conditions infers that, although maximum efficiency of packing the mesogenic groups occurs at approximately 50% added 10PPB2, the mixing achieved with least effort (more spontaneous) is at slightly lower concentrations. From this analysis it is clear that blending the monomer and copolymer is an effective method of increasing the surface mass density of mesogenic

side-chain groups (approximately 12% at 25 °C and 5 mN/m) in the monolayers relative to the pure copolymer films. As alluded to in the Introduction, this may provide a rational means of stabilizing the built-up layer structure in monolayers transferred to solid substrates.

It is also relevant to note here the similarity of the ΔA_{xs} curves for the two-dimensional monolayers of the blends with the thermodynamic phase boundaries obtained for bulk mixtures of the same components. It has been found[10] that the phase diagram of 10PPB2 and 10PPB2-CO has a pronounced minimum of the smectic A–smectic C* phase boundary, the location of the minimum occurring at about 50%. It is interesting that the minima for the ΔA_{xs} versus mole fraction for the monolayers of the blends also occur at the same concentration. These results indicate that the thermodynamics of the mixtures of the copolymer and monomer in their bulk and monolayer states may be similar.

Alternative Analysis of Thermodynamic Data. It has been proposed in a previously published work[22] that the actual limiting packing area of the copolymer is more accurately represented by calculation of the repeat unit as per siloxane unit rather than per mesogenic unit as in the above-mentioned data. This is explained by the additional proposal that the siloxane backbone is at the water surface and is the crucial factor in monolayer behavior due to the similarity of the copolymer monolayer with that of a pure poly(dimethylsiloxane) (PDMS) monolayer. On the basis of the recalculated blend isotherms as compared to initial isotherm values, the true representation of the side-chain copolymer backbone may be somewhere in between the original assumption of the backbone and comonomer units behaving as "spacers" between the mesogens and an extended chain configuration of the siloxane backbone with siloxane monomer units as the close-packing limiting area.

Recalculated ΔA_{xs} versus blend composition plots are shown in Figure 10a. The negative deviation from linearity is still seen, but the minimum is shifted to much smaller 10PPB2 concentrations and its magnitude is smaller. This new representation gives information on the excess area per siloxane unit rather than per mesogen and indicates the largest allowable additional packing of monomer along the backbone is approximately 30%. Assuming there is no difference in attached or added mesogenic groups, this infers a maximum total substitution allowable along the backbone of roughly 60%.

Recalculated ΔG_{mix}^{xs} versus blend composition plots at 25 °C are shown in Figure 10b. The shift and decrease in magnitude of the minimum is similar to that in the recalculated ΔA_{xs} plot described above. The minimum occurs at approximately 20% added monomer concentration and corresponds to the greatest ease of substitution along the backbone occurring at 50% total (attached and added) substitution of mesogen per backbone group.

Brewster Angle Microscopy (BAM). Although the above analyses of the blend isotherms give some general information of the overall behavior of the monolayer films, these methods generally cannot provide insight into the local morphology, such as domain and aggregate formation in two-phase systems and defect topology and tilt variations in liquid crystals. Visualizing some of these features of films during compression has been possible in recent years with the use of fluorescent microscopy.[28,29] However, this method requires, in the case of nonfluorescing materials, the presence of a probe molecule in concentrations as high as 1 mol %. The difficulty in finding a compatible fluorescent marker molecule and the tendency

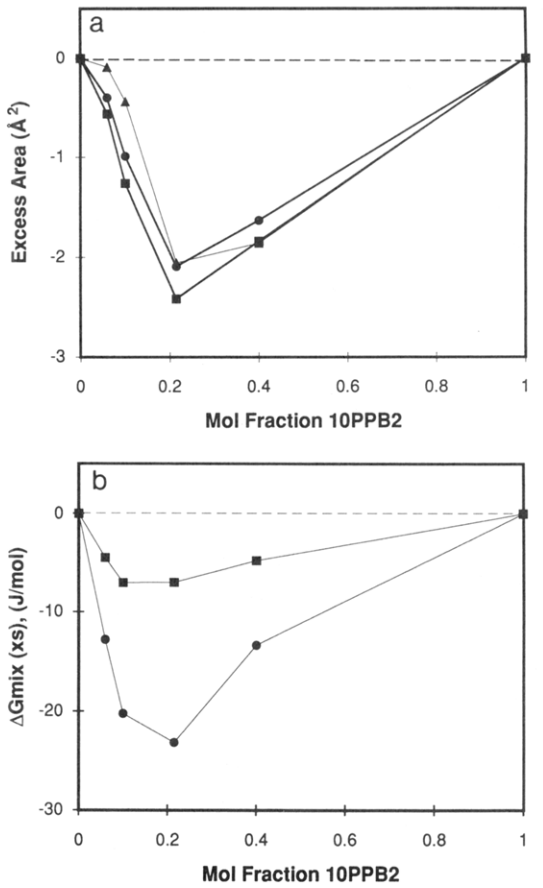

Figure 10. Recalculated plots of ΔA_{xs} (a) and ΔG_{mix}^{xs} (b) versus blend composition at 25 °C.

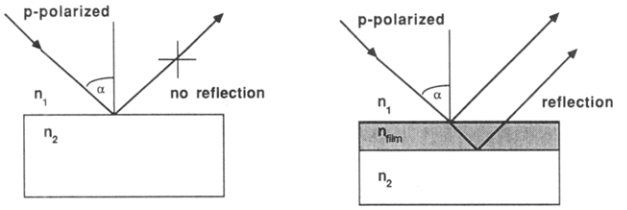

Figure 11. Principle of Brewster angle microscopy.

of such probes to disturb their local environments limit the applications of this method.

Brewster angle microscopy, a method recently developed simultaneously in France[16] and Germany,[17] allows direct visualization of monolayer morphology without the complication of added probe molecules since contrast is dependent upon differences in the refractive indexes of the pure components rather than on emission by excitation of added chromophores. As the accessibility of these instruments increases, BAM measurements may prove to be a more general method to study blends and morphology in monolayers. In order to investigate the local morphology of blend monolayers during compression, Brewster angle microscopy was employed.

When *p*-polarized light is directed at an interface of two materials, as shown in Figure 11, with refractive indices n_1 and n_2, where $n_1 > n_2$, the reflected light intensity is zero at the Brewster angle, α, as defined as

$$\tan \alpha = n_2/n_1$$

When a film possessing a refractive index, n_{film}, different from that of n_2, is introduced to the surface, light is reflected. The Brewster angle microscope images light reflected from an interface. Such changes in the refractive

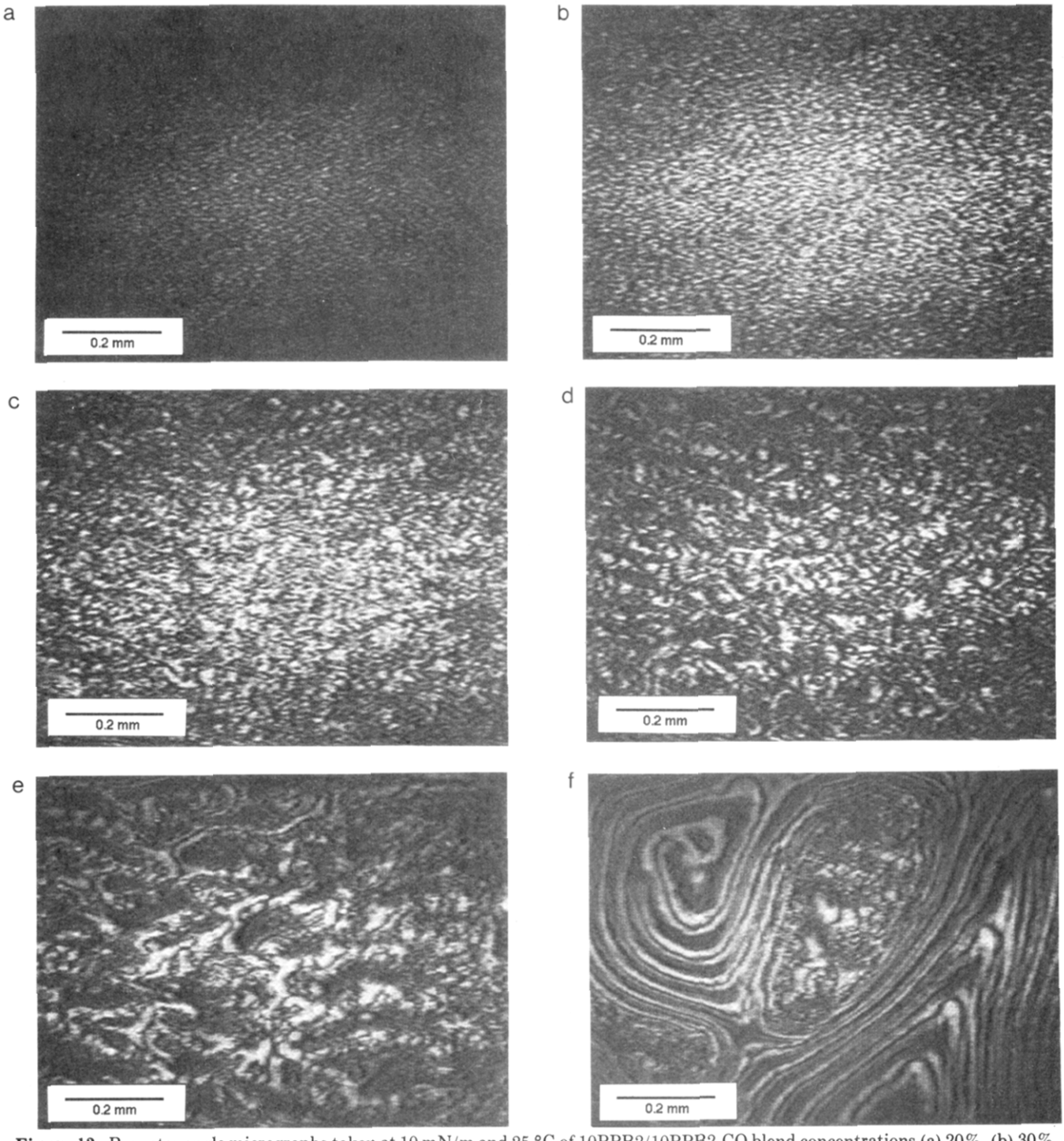

Figure 12. Brewster angle micrographs taken at 10 mN/m and 25 °C of 10PPB2/10PPB2-CO blend concentrations (a) 20%, (b) 30%, (c) 40%, (d) 50%, (e) 70%, and (f) 100%.

index at the interface caused by differences in density, orientation, and aggregation in pure films and phase separation in mixed films are seen as intensity changes in the BAM image. An advantage of this technique is that contrast is obtained without addition of foreign molecules. For the BAM photos shown in Figure 12, an analyzer was placed in front of the CCD camera and set to 90° (analogous to cross polarizers in an optical microscope) so the intensity changes also give information on the extent of orientational order in the monolayer.

The photos of pure 10PPB2-CO are not shown because no morphological features were resolvable in the reflected image at this pressure. A uniform dark image as was seen in 10PPB2-CO at low pressures suggests the lack of birefringence in the monolayers of this copolymer and single phase behavior. As this film is compressed to much higher pressures, a faint granular texture appears which is similar to that seen in the BAM photos of 20% and 30% blends. These granular domains grow brighter as the film is compressed toward a second increase in pressure (around 12 Å^2). A more extensive study of the collapse behavior of this and similar copolymers published by Adams et al.[22] indicates a change in the tilt orientational order and concurrent buildup of smectic layers upon collapse which accounts for the sharp increase in brightness of this region.

In Figure 12, BAM photos of several blend concentrations (20–100 mol % 10PPB2) at 10 mN/m are shown. At this pressure and temperature the blends and pure components are in a similar fluid phase (or below any phase transition). The photos in Figure 12a–e show the

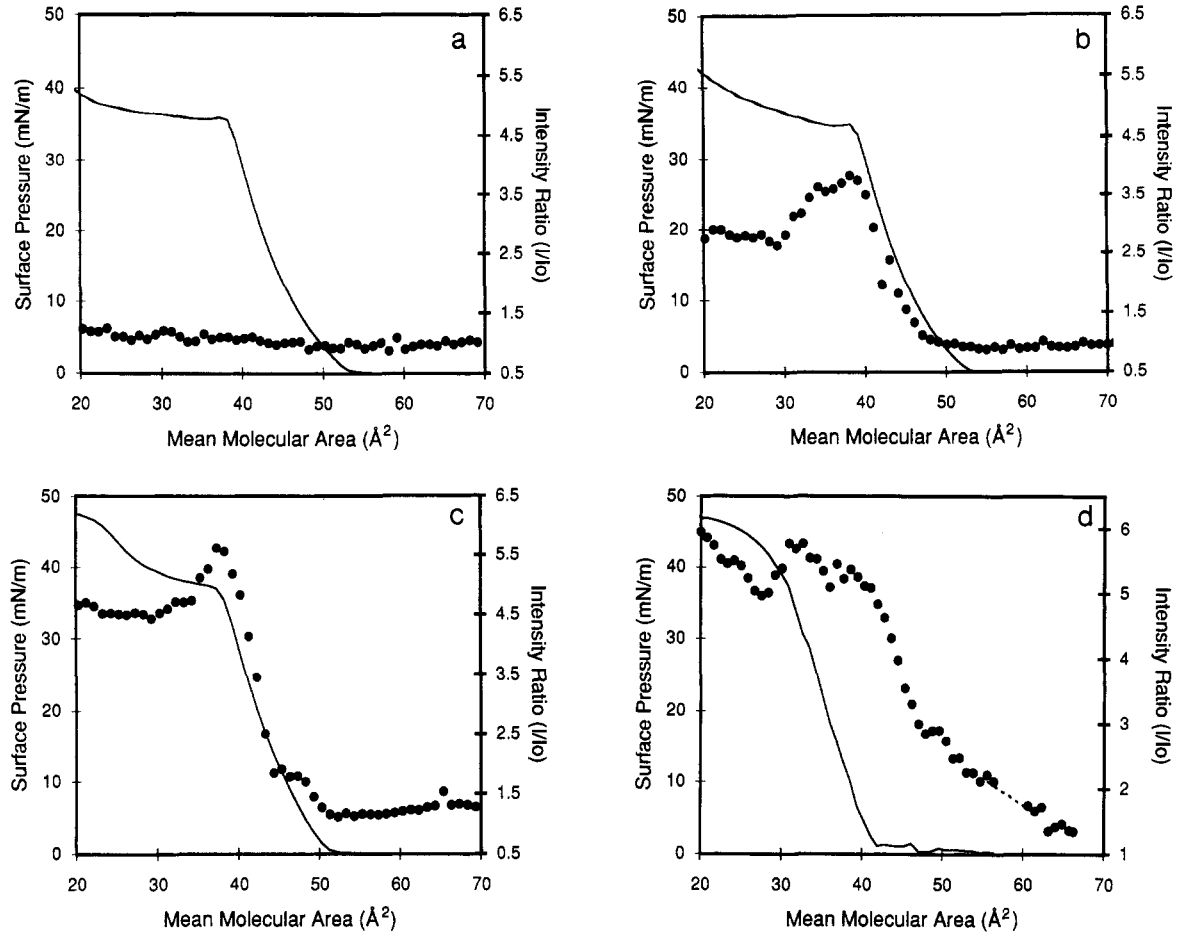

Figure 13. Intensity ratios (I/I_0, where I = integrated intensity at a given area and I_0 = integrated intensity of the clean water phase before spreading the film) and surface pressure versus mean molecular area for (a) 0%, (b) 10%, (c) 20%, and (d) 30% 10PPB2.

progression of morphological features with increasing monomer concentration in the blend monolayers. Areas of similar brightness indicate areas with similar tilt orientational order. It has been proposed that the unusual striped textures of the monomer (Figure 12f) are due to defects caused by fluctuations of $\hat{n}$, the projection of the tilt director of the mesogenic group on the layer plane,[30] as is seen in chiral smectic free-standing films.[31] Smaller and less organized structures emerge in the 40% blend film photo. These textures are all in agreement with a single phase with variations in mesogen tilt degeneracy. Granular structures which constitute regions over which the tilt order is coupled increase in size and are evident in a type of a schlieren texture at 50% and 70%. Even at 70%, however, there are no large areas of the striped domains seen in the monomer.

The pure monomer monolayer film shows fluid birefringent domains separated by disordered or dark regions at high surface areas (observed up to 90 Å²) which correspond to a liquid or liquid crystalline–gas coexistence region. The characteristic birefringent fluid striped texture as shown in Figure 12f appears from the surface pressure onset up to the liquid-condensed transition region. However, at room temperature the bulk monomer is crystalline. At the water surface, the hydration interaction and lowering of the water surface energy are thus sufficient to keep the monomer as an ordered liquid in the monolayer rather than a condensed crystalline phase seen in the bulk. Yet this effect is not sufficiently strong enough to disrupt the monomer–monomer cohesive forces to form the disordered isotropic phase seen in the copolymer.

The above results show a homogeneous dispersion of the polymer content in the blends. More importantly, the results show the significant effect of the polymer disrupting long-range tilt interactions in the monolayer. This is not surprising since the "meandering" path of the polymer backbone on the water surface would affect the local tilt directors of the side groups. It would be of considerable interest to probe the difference in the extent of tilt order of the blends in the monolayer and bulk states. As such, this may be an interesting example of a polymer used to plasticize a low molecular weight compound.

BAM Intensity Measurements. In the BAM experiments, the amount of light reflected while the analyzer is in place in front of the CCD camera is an indication of the orientational order or birefringence in the films. This is presented as the intensity ratio, the integrated intensity captured by the camera at a given pressure during monolayer compression (I) relative to that of a pure water surface (I_0). Plots of the intensity ratio (I/I_0) and surface pressure versus mean molecular area for various blend concentrations are shown in Figure 13. In the plots for 0–30%, all settings including intensity gain were held identical, for the purpose of comparison.

Curve a shows the intensity plot for the pure copolymer. As was stated earlier the intensity does not significantly increase until elevated pressures, indicating a lack of long-range orientational order until further smectic multilayer buildup. The combination of the lack of birefringent reflectance and the significant pressure increase infers an isotropic liquid-like monolayer phase. As in the monomer film, this indicates that the monolayer film is one step further disordered than the corresponding bulk phase, which under these conditions for the copolymer is in a smectic C* liquid crystalline phase. This is thought to be caused by the interaction of the polysiloxane backbone

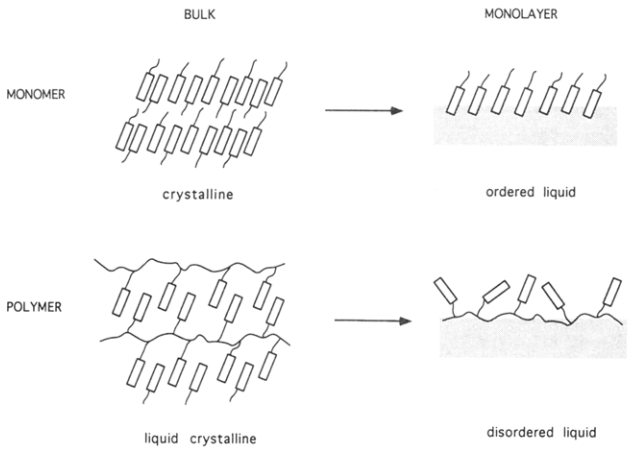

Figure 14. Differences in theoretical packing of mesogenic groups in the bulk and monolayer of 10PPB2 and 10PPB2-CO.

with the water surface resulting in two net effects. First, the hydration of the backbone in the water surface extends the chain and increases the distance between mesogenic groups sufficiently to prevent interaction. Second, the water surface acts as an external field, which coupled with the weak amphiphilic character of the copolymer causes all side groups to point away from the water surface. This tends to prevent the antiparallel packing of the mesogens necessary for the ordering observed in the bulk (see Figure 14). Compared to the monomer behavior both in the bulk and at the air–water interface, the addition of a polymer backbone acts to produce additional disorder among the liquid crystalline mesogens in the copolymer.

In Figure 13, curves b–d show intensity ratio plots for the blends. The curves all show an intensity increase at or before the onset of a surface pressure increase. As shown in curve b, with only 10% addition of monomer, intensity increases in magnitude and onset mean molecular area. Although the shape of the 20% curve is similar to that of the 10% curve, the maximum intensity is greater, suggesting a greater concentration of molecules with the same orientational ordering. The onset area of the 20% curve is also shifted to somewhat higher values. A further intensity ratio increase is seen in the 30% concentration as well as an earlier onset surface area. Plots of the 40% and higher concentrations were not shown due to a high noise level in the intensity ratio values as aggregates floated in and out of the field of view at high mean molecular area.

The above results suggest that blending the monomer with the copolymer has two effects. First, by adding monomer, a greater concentration of mesogenic units show long-range orientational ordering (the lateral resolution of the BAM is estimated to be about 10 μm). Second, by adding monomer, the onset of orientational ordering shifts to higher surface areas, surpassing the surface pressure onset point. This interpretation, in agreement with much of the previous data, indicates attractive interactions between mesogens of the monomer and copolymer, as well as more efficient packing of these side groups and mesogens.

Conclusions

There are a number of methods to analyze the miscibility in mixed monolayers at an air–water interface. Although most methods are not conclusive when viewed alone, several methods employed which yield similar results are very convincing. Additionally, the results from these analyses can give further information as to the type of interaction within the films and characteristics of the

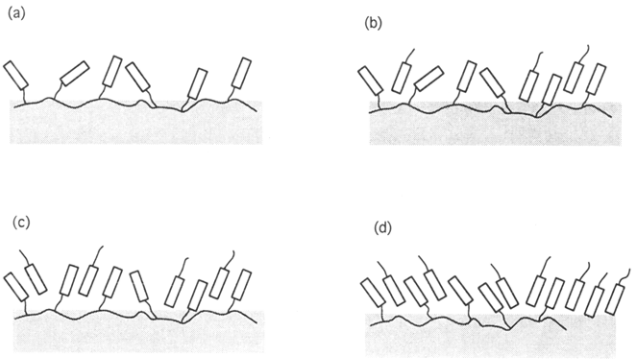

Figure 15. Proposed packing of mesogens in pure films and blends.

resulting blend films. The results for the 10PPB2-CO/10PPB2 blends may be summarized as follows:

(i) Decreased compressibility of the blend films relative to the pure compounds indicated not only that it was a miscible system but also that there were attractive forces between two components to cause such a decrease.

(ii) An increase in the collapse pressure also indicates positive interaction between components, creating a more coherent blend monolayer which is more resistant to collapse.

(iii) Excess area values give a maximum efficiency of packing of the blends as 50% added monomer to copolymer mesogenic group and in recalculated data 30% added monomer per siloxane unit in the copolymer.

(iv) Excess free energy of mixing values show not only that the blends are miscible but also that the most spontaneous mixing occurs at approximately 40% added 10PPB2 to copolymer mesogen and 20% added per siloxane unit in the copolymer.

Based on the above conclusions, the large mean molecular area occupied by the copolymer mesogens, and the lack of birefringent intensity seen in the isotherms of the copolymer, the packing of 10PPB2-CO and blend films at the air–water interface is proposed as shown in Figure 15. Recalculated thermodynamic isothermal data indicate that the backbone is far more crucial in the monolayer packing than was initially presumed. The extension of the siloxane backbone and its probable interaction with the water surface prevent any extensive interaction between the side-chain mesogenic groups in the pure copolymer films. Additionally, the lack of birefringence seen in BAM intensity data of the 10PPB2-CO films confirms that there is little long-range correlation between the side group mesogens such as that seen in the monomer. Due to the large area and the probable existence of gaps between the mesogens in the copolymer, the mesogen may be accommodated within the packing confines of the copolymer up to a certain percent composition. However, above this loading capacity the excess monomer would be squeezed out or initially excluded from the polymer packing area. Although evenly dispersed among the copolymer/monomer areas, the excess monomers appear to organize on a small scale as they would in pure monomer film.

Acknowledgment. Dr. Jawad Naciri at Naval Research Laboratories, Washington, DC, is acknowledged for the syntheses of all compounds presented in this work. Dr. John Ruth, also from Naval Research Laboratories, is acknowledged for data and results on the bulk blends. Dr. Jörg Adams is thanked for his assistance with the Brewster angle microscope reflectivity measurements and integration of the data. The authors acknowledge the NSF-sponsored REU site at the University of Florida

(Grant CHE-9200344) for financial assistance for Mr. U. Rädler. KSV Instruments (Helsinki, Finland) is acknowledged for technical assistance with the Langmuir–Blodgett equipment and software.

References and Notes

(1) Collet, P. *J. Phys. Radium* **1922**, *3*, 128.
(2) Leathes, J. B. *Lancet* **1925**, *1925*, 853.
(3) Gaines, G. L. *Insoluble Monolayers at Liquid–Gas Interfaces*; John Wiley & Sons: New York, 1966.
(4) Baglioni, P.; Dei, L.; Gabrielli, G.; Innocenti, F. M.; Niccolai, A. *Colloid Polym. Sci.* **1988**, *266*, 783.
(5) Caminati, G.; Gabrielli, G.; Puggelli, M.; Ferroni, E. *Colloid Polym. Sci.* **1989**, *267*, 237–245.
(6) Puggelli, M.; Gabrielli, G. *Colloid Polym. Sci.* **1983**, *261*, 166–170.
(7) Rapp, B.; Eberhardt, M.; Gruler, H. *Makromol. Chem. Macromol. Symp.* **1990**, *46*, 439.
(8) Penner, T. L.; Schildkraut, J. S.; Ringsdorf, H.; Schuster, A. *Macromolecules* **1992**.
(9) Thibodeaux, A. F.; Geer, R.; Qadri, S.; Naciri, J.; Shashidhar, R.; Duran, R. S. *Polym. Prepr. (Am. Chem. Soc., Div. Polym. Chem.)* **1992**, *33*, 1220.
(10) Ruth, J.; Naciri, J.; Shashidhar, R. *Liq. Cryst.*, in press.
(11) Matsumoto, M.; Miyasaka, H.; Sekiguchi, T.; Tanaka, M.; Tachibana, H.; Nakamura, T.; Manda, E.; Kawabata, Y. *Thin Solid Films* **1989**, *178*, 367.
(12) Büschl, R.; Hupfer, B.; Ringsdorf, H. *Makromol. Chem., Rapid Commun.* **1982**, *3*, 589.
(13) Bacon, K. J.; Barnes, G. T. *J. Colloid Interface Sci.* **1978**, *67*, 70.
(14) Ruiz, M. J. G.; Vilchez, M. A. C. *Colloid Polym. Sci.* **1991**, *269*, 77.
(15) Petrov, J. G.; Möbius, D.; Angelova, A. *Langmuir* **1992**, *8*, 201.
(16) Hénon, S.; Meunier, J. *Rev. Sci. Instrum.* **1991**, *62*, 936.
(17) Hönig, D.; Möbius, D. *J. Phys. Chem.* **1991**, *95*, 4590.
(18) Naciri, J.; Pfeiffer, S.; Shashidhar, R. *Liq. Cryst.* **1991**, *10*, 585.
(19) Adams, J.; Thibodeaux, A.; Naciri, J.; Shashidhar, R.; Duran, R. S. *Polym. Prepr. (Am. Chem. Soc., Div. Polym. Chem.)* **1992**, *33*, 1164.
(20) Rettig, W.; Naciri, J.; Shashidhar, R.; Duran, R. S. *Thin Solid Films* **1992**, *210*, 114.
(21) Rettig, W.; Naciri, J.; Shashidhar, R.; Duran, R. S. *Macromolecules* **1991**, *24*, 6539.
(22) Adams, J.; Buske, A.; Duran, R. S. *Macromolecules*, in press.
(23) George, L.; Gaines, J. *Langmuir* **1991**, *7*, 834.
(24) Crisp, D. J. *Research (London), Suppl.* **1949**, *23*, 65.
(25) George, L.; Gaines, J.; Bellamy, W. D.; Tweet, A. G. *J. Chem. Phys.* **1964**, *41*, 538.
(26) George, L.; Gaines, J. *J. Chem. Phys.* **1978**, *69*, 924.
(27) Goodrich, F. C. *Proceedings 2nd International Congress on Surface Activity*; 1957; Vol. 1.
(28) Möhwald, H. *J. Mol. Electron.* **1988**, *4*, 47.
(29) Duschl, C.; Kemper, D.; Frey, W.; Meller, P.; Ringsdorf, H. *J. Phys. Chem.* **1989**, *93*, 4587.
(30) Adams, J.; Rettig, W.; Duran, R. S.; Naciri, J.; Shashidhar, R. *J. Phys. Chem.* **1993**, *97*, 2021.
(31) Takanishi, Y.; Takezoe, H.; Fukuda, A. *Phys. Rev. B* **1992**, *45*, 7684.